ISSN 1063-7761, Journal of Experimental and Theoretical Physics, 2011, Vol. 113, No. 2, pp. 181–191. © Pleiades Publishing, Inc., 2011.
Original Russian Text © V.E. Zobov, V.P. Shauro, 2011, published in Zhurnal Eksperimental'noi i Teoreticheskoi Fiziki, 2011, Vol. 140, No. 2, pp. 211–223.

ATOMS, MOLECULES, OPTICS

On Time-Optimal NMR Control of States of Qutrits Represented by Quadrupole Nuclei with the Spin $I = 1$

V. E. Zobov* and V. P. Shauro

L.V. Kirensky Institute of Physics, Siberian Branch, Russian Academy of Sciences, Krasnoyarsk, 660036 Russia

e-mail: rsa@iph.krasn.ru

Received November 10, 2010

Abstract—Elementary logical operators (selective rotation, Fourier transform, controllable phase shift, and SUM gate) are considered for a quantum computer based on three-level systems (qutrits) represented by nuclear spins $I = 1$ under nuclear magnetic resonance conditions. The computer simulation of the realization of these operators by means of simple and composite selective radiofrequency (RF) pulses and optimized RF pulses is performed. The time dependence of the amplitude of last pulses is found by numerical optimization at different durations. Two variants are proposed for realization of a two-qutrit SUM gate by using one-qutrit or two-qutrit optimized RF pulses. The calculated time dependences of realization errors were used to study the time optimality of different methods for obtaining gates, proposed earlier and in this paper. The advantages and disadvantages of each of the methods are evaluated for different values of physical parameters.

DOI: 10.1134/S1063776111060094

1. INTRODUCTION

The use of multilevel quantum systems as basic elements in quantum computations promises a number of advantages. First, when a quantum algorithm is implemented by applying one- or two-qubit elementary logical operators (gates) successively in time to a system of working qubits, the number of gates can be reduced by inserting a multilevel particle, for example, a three-level particle instead of a two-level particle [1, 2]. Second, in another possible method of algorithm implementation [3–7]—in which a qubit register (counter or cursor) that enumerates operations is added and the Hamiltonian of the system is written as the sum of the products of Hamiltonians of individual gates by an operator that changes the counter state, three-particle large-radius interaction between qubits from different registers is required as a minimum. It is possible to return to the common nearest-neighbor pair interaction by passing to multilevel particles and virtually realizing working qubits and counter qubits at different levels of the same particle [3–7]. Third, the preparation of a stable initial state for quantum calculations by successive measurements can be more simply performed for multilevel systems than for two-level systems [8]. Finally, calculations with qudits (quantum systems with d levels) require a smaller number of elements to obtain the needed size of the calculation basis [9–12]. The next element after a qubit in the number of levels is a qutrit having three states. By implementing quantum algorithms based on qutrits, one can pass from the binary system to the ternary system and use its advantages [12–14].

It is known [15–17] that any quantum algorithm can be implemented by using a sequence of one- and two-qutrit gates [9, 10, 16, 18, 19]. Therefore, it is necessary to be able to realize such gates on different physical systems. By now this problem is far from being completely solved. In this paper, we chose as qutrits quadrupole nuclei with spin $I = 1$ controlled by a radiofrequency (RF) magnetic field under NMR conditions [20]. In a strong static magnetic field and an inhomogeneous electric field, a nucleus has three nonequidistant energy levels separated by intervals $\hbar(\omega_0 \pm q)$, where ω_0 is the Larmor frequency and q is the quadrupole interaction constant. The NMR spectrum is a doublet with splitting $2q$ caused by the selection rule, admitting only transitions accompanied by a change in the spin projection by unity. An example is the deuterium nucleus on which one-qutrit gates were realized [21]. To realize two-qutrit gates, we assume the presence of a weak spin–spin interaction. The aim of our study (numerical simulations) was to find the basic rules for controlling multilevel systems and primarily compare experimental times for different methods of gate realization because, to successfully perform an experiment on a real setup, it is necessary to have time to use the entire sequence of gates for a time shorter than the relaxation (decoherence) time of the system.

The most direct method to control the state of a quadrupole nucleus involves the use of selective RF pulses with a frequency equal to that of the required transition and a small amplitude $\omega_{rf} \ll q$. Quantum computations on one quadrupole nucleus using selective Gaussian pulses were performed, for example, in [21–26]. The state of a quadrupole nucleus can be also

transformed by means of an RF pulse with a harmonically modulated amplitude [25–28]. The frequencies of harmonics are set equal to transition frequencies, while their amplitudes are specified according to the required transformation, for example, the transformation of the equilibrium state to the effectively pure state. At present, to ensure a long enough decoherence time, quantum NMR computations are realized in a liquid-crystal phase where thermal motions average the inhomogeneities of magnetic fields and intermolecular interactions, resulting in NMR spectra consisting of very narrow lines. The same motions strongly weaken quadrupole and intramolecular dipole–dipole interactions. As a result, the duration of selective pulses increases, but the additional possibility appears for control by high-power nonselective RF pulses [21, 24].

Recently we proposed using sequences of nonselective RF pulses separated by free evolution intervals with quadrupole interaction for performing composite selective rotations between two neighboring levels of a quadrupole nucleus [29, 30]. The minimum duration T_∞ of such a composite operator was found, which is equal to the total duration of free evolution intervals. It was shown theoretically that for duration T of composite operators exceeding T_∞, the rotation error can be made arbitrarily small, whereas for $T < T_\infty$, the error remains finite.

Currently, the state of quadrupole nuclei is controlled using optimization methods in which the time dependences of the amplitude and phase of a RF pulse are found numerically from the condition of ensuring minimal error in the realization of the specified unitary transformation. For example, in [31] the problem of optimal excitation of three-quantum transitions in the ^{87}Rb quadrupole nucleus ($I = 3/2$) was solved for rotation at the magic angle. The authors performed calculations by the GRAPE (gradient ascent pulse engineering) optimization method [32]. Then, this method was applied in [33, 34] to excite the central transition in ^{23}Na quadrupole nuclei ($I = 3/2$). In [34], the modified Krotov optimization method, ensuring better convergence of iterations, was proposed to solve the same problem. Finally, the spin quantum state in the ^{23}Na nucleus in a single crystal [35] and a liquid crystal [36] was transformed using a so-called strongly modulated pulse consisting of several RF pulses with characteristics selected by the numerical optimization method proposed in [37].

In this study, we used the GRAPE optimization method to perform quantum computations on quadrupole nuclei with the spin $I = 1$. We calculated optimized RF pulses for one-qutrit gates of selective rotations, the quantum Fourier transform (QFT), and for the two-qutrit SUM gate [10, 16, 18, 19, 38]. Calculations were performed for different pulse durations. As in [32], we used the time dependences of the error to study the time optimality of the gate realization methods proposed earlier such as composite selective rotation [29, 30], the QFT, and the SUM gate obtained with the help of RF pulses selective in the quadrupole or spin–spin splitting of the NMR line [38]. The shape of the control RF field for realization of the SUM gate was calculated using the GRAPE algorithm according to two schemes: first, directly up to the total unitary operator with the 9×9 matrix and, second, by means of optimized RF pulses for one-qutrit gates with 3×3 matrices. The second variant is important because it can be applied to multiqutrit systems, since, as was pointed out in [39] with the example of multiqubit systems, optimization over the total basis is an exponentially complex problem. We studied the dependences of gate errors on physical parameters and gave recommendations for their realization.

2. ONE-QUTRIT GATES

2.1. Control Theory

Consider a quadrupole nucleus with spin $I = 1$ placed in a strong static magnetic field B_0 and a control RF magnetic field B_{rf}. In a reference frame rotating around the constant field direction (z axis) at the RF field frequency ω_{rf} [20], the Hamiltonian of our model takes the form

$$H(t) = -(\omega_0 - \omega_{rf})I_z + q(I_z^2 - 2/3) + u_x(t)I_x + u_y(t)I_y. \quad (1)$$

Here, $\omega_0 = \gamma B_0$ is the Larmor frequency, I_α is the spin projection operator on the α axis, q is the constant of the quadrupole interaction of the nucleus with the gradient of the axially symmetric crystal field, and $u_\alpha(t)$ is the frequency equal to the product of the gyromagnetic ratio γ by the projection of the RF control field B_{rf} on the α axis ($\alpha = x, y$), which for brevity we will call the RF field amplitude. Energy will be also measured in frequency units, assuming that $\hbar = 1$. In the absence of RF field, the system has three nonequidistant energy levels

$$\lambda_0 = -\omega_0 + q/3, \quad \lambda_1 = -2q/3, \quad \lambda_2 = \omega_0 + q/3,$$

for the states with different values of I_z

$$|I_z = 1\rangle = |0\rangle, \quad |I_z = 0\rangle = |1\rangle, \quad |I_z = -1\rangle = |2\rangle. \quad (2)$$

We use them as the computation basis for a qutrit.

To realize quantum computations, it is necessary to find the control field in such a way that the evolution operator

$$U(T) = \hat{D}\exp\left(-i\int_0^T H(t)dt\right) \quad (3)$$

performs for time T some logical unitary transformation of the qutrit state specified by a 3×3 matrix in computation basis (2). Here, $\hat{D}$ is the time-ordering operator.

For example, a one-qutrit gate of selective rotation through angle θ in the transition between the $|0\rangle$ and $|1\rangle$ states is represented by the matrix

$$R_\alpha^{0-1}(\theta) = \begin{bmatrix} \cos\frac{\theta}{2} & -ie^{-i\varphi}\sin\frac{\theta}{2} & 0 \\ -ie^{i\varphi}\sin\frac{\theta}{2} & \cos\frac{\theta}{2} & 0 \\ 0 & 0 & 1 \end{bmatrix}. \quad (4)$$

The parameter φ determines the direction of the rotation axis in the *xy* plane in the reference frame. Thus, for $\varphi = 0$, rotation is performed around the *x* axis ($\alpha = x$), and for $\varphi = \pi/2$ around the *y* axis ($\alpha = y$).

Selective rotation (4) around the *y* axis can be performed using a rectangular RF pulse $u_x(t) = 0$, $u_y(t) = \Omega$ with frequency $\omega_{rf} = \omega_0 - q$ and duration

$$T_p = \frac{\theta}{\Omega\sqrt{2}}. \quad (5)$$

To obtain selective rotation with a high precision, the inequality $\Omega \ll q$ should be fulfilled because at large field amplitudes not only the resonance transition will be excited. The rotation error can be decreased by choosing a more complex pulse shape, for example, Gaussian. At present various numerical methods are used to find the optimal shape of RF pulses.

A search for the control RF field by means of the optimization GRAPE algorithm [32] is performed by iterating the amplitude $u_\alpha(t)$ to maximize the performance function

$$\Phi = \left|\mathrm{Sp}\{U_0^* U(T)\}\right|^2 / \{\mathrm{Sp}(1)\}^2$$

and minimizing, correspondingly, the error of the obtained gate:

$$\Delta = 1 - \Phi. \quad (6)$$

Here, $U(T)$ is the matrix of evolution operator (3) during time T and U_0 is the matrix of the ideal transformation to be obtained. The time interval T is divided into N equal segments with duration $\Delta t = T/N$, the field amplitude in each *j*th segment being constant and equal to $u_\alpha(t_j)$, where $t_j = j\Delta t$ and $j = 1, 2, \ldots, N$. The calculation of the gradient $\delta\Phi/\delta u_\alpha(t_j)$ by expressions from [32] gives new values of $u_\alpha(t_j)$ $\alpha = x, y$ for the next iteration of the algorithm:

$$u_\alpha(t_j) \longrightarrow u_\alpha(t_j) + \varepsilon\frac{\delta\Phi}{\delta u_\alpha(t_j)},$$

where ε is a small parameter. Calculations stop when the difference of errors (6) in the last two iterations becomes smaller than some value (on the order of 10^{-10} in our calculations). Note also that we imposed no restrictions on the control field amplitude and shape.

2.2. Selective Rotations

By using the GRAPE algorithm, we calculated $u_\alpha(t)$ for selective rotations $R_y^{0-1}(\theta)$ through angles $\pi/4$, $\pi/2$, $3\pi/4$, and π for different pulse durations T. The control RF field was tuned to the central frequency $\omega_{rf} = \omega_0$, and a small-amplitude rectangular pulse was used as the initial condition. The calculation results are presented in Figs. 1–3. Figure 1 shows that error Δ (6) drastically increases with decreasing the pulse duration below some value T_m depending on the rotation angle θ. The value of T_m is close to the theoretical value $T_\infty = 3\theta/2\sqrt{2}\,q$ obtained in [29, 30] for a composite selective pulse. We do not present here the results for selective RF pulses of the determined shape (rectangular or Gaussian) because at the time scale under study they lead to errors greater by a few orders of magnitude [29, 30, 40, 41].

Recall that a composite selective rotation through angle θ for the time T was performed in [29, 30] with the help of the effective Hamiltonian H_{eff} obtained from H_q [see the second term in (1)] under the action of intense nonselective RF pulses. In particular, it was found for $R_y^{0-1}(\theta)$

$$TH_{eff} = \exp\left(\frac{i\pi I_x}{4}\right)(H_q t_1)\exp\left(-\frac{i\pi I_x}{4}\right) + \exp\left(-\frac{i\pi I_y}{2}\right)(H_q t_2)\exp\left(\frac{i\pi I_y}{2}\right) + \eta I_y, \quad (7)$$

where $t_1 = 2t_2 = \theta/q\sqrt{2}$ and $\eta = \theta/2\sqrt{2}$. For comparison, Fig. 1 shows the error for composite selective-rotation pulses obtained from Hamiltonian (7) and simulated in the strong RF field $\Omega \gg q$. The relation between the RF-field amplitude and the composite pulse duration is determined by the expression

$$\Omega = \frac{\theta/2\sqrt{2} + 2\pi N_c}{T - T_\infty}, \quad (8)$$

where N_c is the number of cycles in the Trotter–Suzuki expansion, which is used to improve the accuracy of the construction of effective Hamiltonian (7) from the noncommuting operators of the composite pulse. The value of T_∞ is determined by the duration of free-evolution intervals in the composite pulse

$$T_\infty = t_1 + t_2 = \frac{3\theta}{2\sqrt{2}q}. \quad (9)$$

It follows from our results that for $T > T_\infty$ the selective rotation error can be made arbitrarily small by increasing N_c. However, in this case, it is necessary to increase the total number of nonselective RF pulses $N_S = 7N_c$ and their amplitude Ω. As Ω is decreased, the error increases due to the violation of the ideality of nonselective rotations caused by the quadrupole interaction. This error can be decreased by replacing simple non-

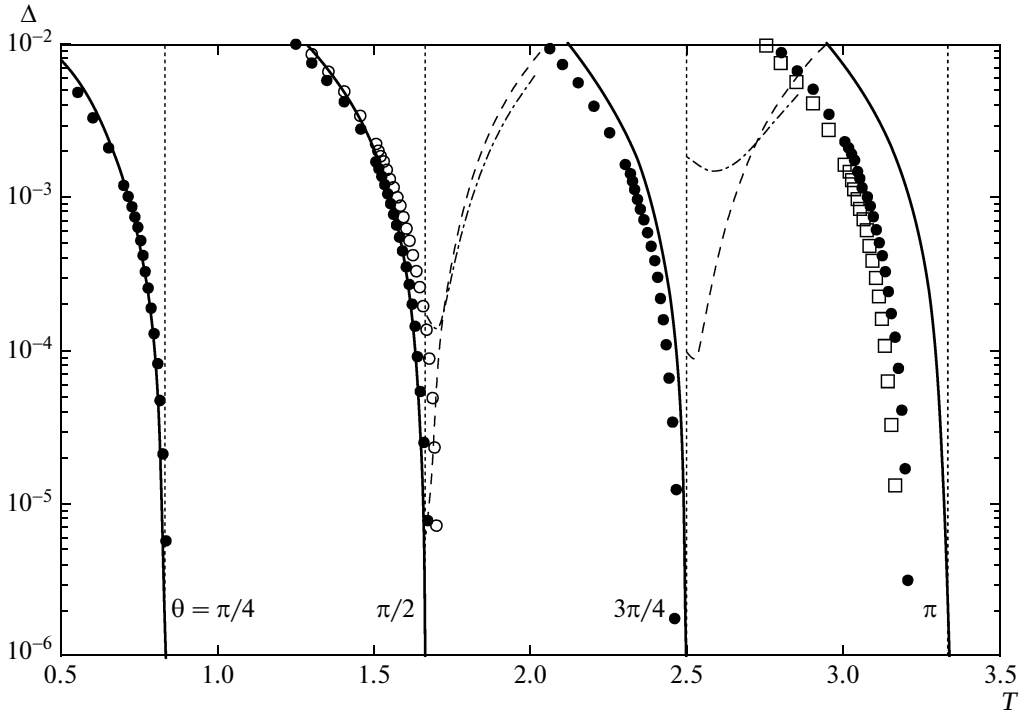

Fig. 1. Dependences of error (6) for the operator $R_y^{0-1}(\theta)$ on the optimized pulse duration T (in $1/q$ units) for different values of θ. The values of Δ are calculated for the partition numbers $N = 100$ (□), 50 (●), and 30 (○). The vertical dotted straight lines correspond to times T_∞ (9). The solid curves show theoretical estimates of error (10) for corresponding rotation angles. The dependences of the error for pulsed sequences from [30] are shown by dot-and-dash curves for $N_c = 1$ and dashed curves for $N_c = 2$.

selective RF pulses by a more complicated sequence of pulses [30], but such a replacement leads to an increase in the total duration of the operation.

In the limit $\Omega \longrightarrow \infty$, the time of selective rotation produced by a composite pulse is $T = T_\infty$. If this time in effective Hamiltonian (7) is decreased to $T = xT_\infty = 3x\theta/2\sqrt{2}\,q$ ($x \in [0, 1]$), the ideal selective rotation will not be achieved. In this case, the error for operator (4) will be ascribed by the expression

$$\Delta = 1 - \frac{1}{9}\left[\frac{a^2}{A^2} + \left(1 + \frac{a^2}{A^2}\right)\cos\frac{\theta}{2}\cos\frac{\theta A}{2} + \frac{b^2}{A^2}\left(\cos\frac{\theta}{2} + \cos\frac{\theta A}{2}\right) + \frac{2a}{A}\sin\frac{\theta}{2}\sin\frac{\theta A}{2}\right]^2, \quad (10)$$

where $a = (1 + x)/2$, $b = (1 - x)/2$, and $A^2 = a^2 + b^2$. Note that error (10) is caused by the distortion of effective Hamiltonian (7) itself rather than by the use of the Trotter–Suzuki expansion for noncommuting operators (i.e., it corresponds to the limit $N_c \longrightarrow \infty$, whereas the error will be greater for a finite value of N_c). One can see from Fig. 1 that dependence (10) well describes numerical results obtained by the GRAPE method for angles $\theta = \pi/4$ and $\pi/2$. For greater rotation angles, the optimized pulse is realized with the same error for a shorter time (by 7% for the angle π). This is probably explained by the fact that the RF field in the optimized pulse acts simultaneously with H_q, whereas in the case of the ideal composite pulse, this field acts successively. Therefore, the GRAPE algorithm for the optimized pulse finds the time dependence of the RF field at which the quadrupole interaction does not prevent the fulfillment of the specified operation, but on the contrary, facilitates it. Due to such a consistent consideration of the simultaneous action of H_q and $H_{\rm rf}$, the high efficiency is achieved.

The shape of optimized pulses for $\theta = \pi/2$ is shown in Fig. 2. As the pulse duration is deceased, the average amplitude of the RF field increases. The shape of the optimized pulse weakly depends on the initial condition for $T \le T_m$, whereas for $T > T_m$, different pulses can be obtained which lead to a very small error. As the partition number N of the time interval is increased, the pulse shape changes insignificantly and the error tends to a limiting value, as is seen for the π pulse in Fig. 3. For small N, the shape and average amplitude of the RF field can noticeably change due to a poor stability of the algorithm when the condition $\Delta t \ll \|H\|^{-1}$ is violated [32].

The RF-field amplitudes of optimized pulses are many times smaller than values (8) for the same durations. Thus, it follows from Figs. 1 and 2 that already

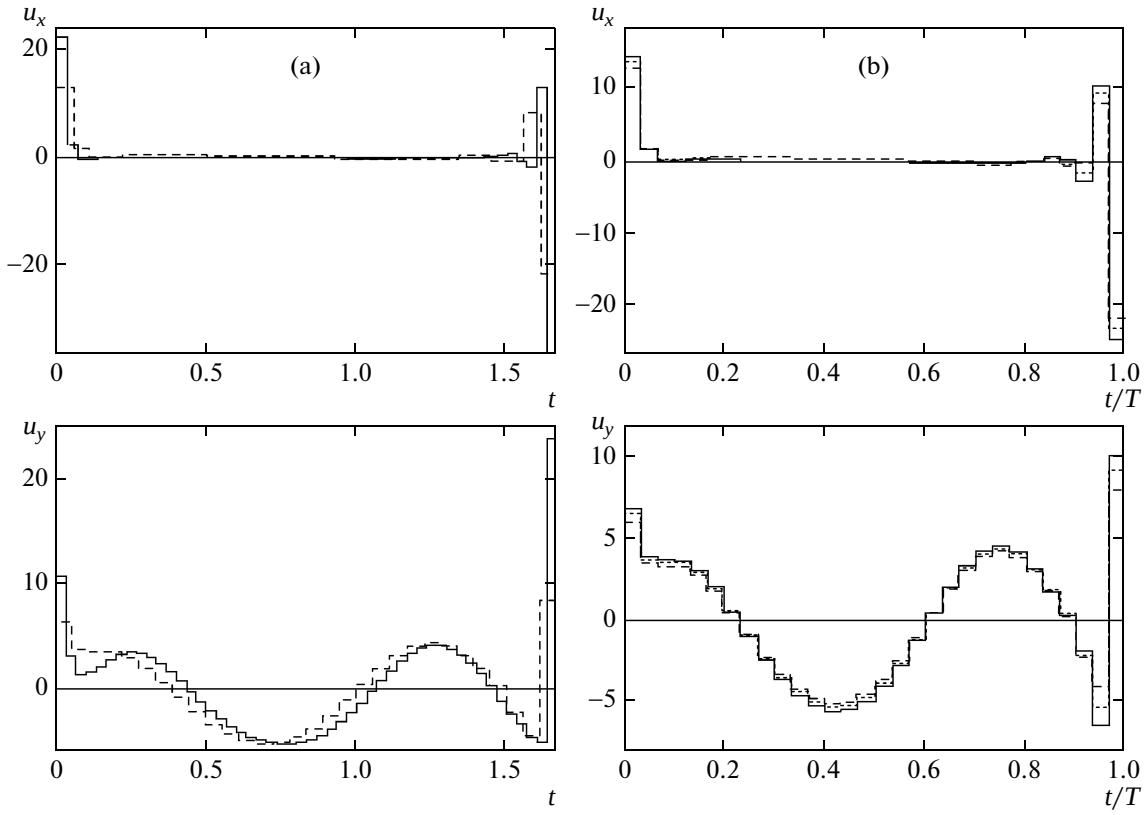

Fig. 2. Change in the shape of the optimized RF pulse for the operator $R_y^{0-1}(\pi/2)$ for (a) the duration $T = 1.67$ and $N = 50$ (solid curves), 30 (dashed curves) and (b) $N = 50$ and $T = 1.5$ (solid curves), 1.6 (dotted curves), and 1.7 (dashed curves). Amplitudes and time are measures in units q and $1/q$, respectively.

for $N = 30$ the optimized pulse with the modulus of the RF-field amplitude not exceeding $23q$ performs rotation through $\pi/2$ for the time $T = 1.69/q$ with the same error as for a composite pulse consisting of 14 pulses with the amplitude $550q$.

We do not consider other selective rotation operators [29] because the results for them are qualitatively the same.

Note that the GRAPE method was applied in [40, 41] to the three-level system of a superconductor for solving a principally different problem of eliminating the error from the third level upon controlling a qubit at two levels. In [41], the control-field frequency was selected equal to the resonance frequency of an individual transition in the three-level system (optimization of the selective pulse), whereas in our case, $\omega_{rf} = \omega_0$. Both variants are admissible when a large-amplitude RF field required for decreasing the pulse duration is used. Our tuning to the central frequency is more universal because it provides the control of all transitions with the help of a RF field at one frequency, for example, upon performing the QFT at three levels.

2.3. Computation of an Optimized QFT Pulse

To perform the QFT of a qutrit, selective rotations should be disposed successively in time according to the scheme [42]

$$F = iR_y^{1-2}\left(-\frac{\pi}{2}\right)R_y^{0-1}(-2\arctan\sqrt{2}) \times R_z^{0-1}(\pi)R_y^{1-2}\left(\frac{\pi}{2}\right) \quad (11)$$

$$= \frac{1}{\sqrt{3}}\begin{bmatrix} 1 & 1 & 1 \\ 1 & \frac{-1-i\sqrt{3}}{2} & \frac{-1+i\sqrt{3}}{2} \\ 1 & \frac{-1+i\sqrt{3}}{2} & \frac{-1-i\sqrt{3}}{2} \end{bmatrix}.$$

If the sequence of selective rotations (11) is realized by means of the optimized pulses described above and their duration is approximately estimated by the value of T_∞, the total QFT duration is $5.36/q$ when z rotation is performed by the RF-field phase shift or $12.02/q$ when the composite z rotation

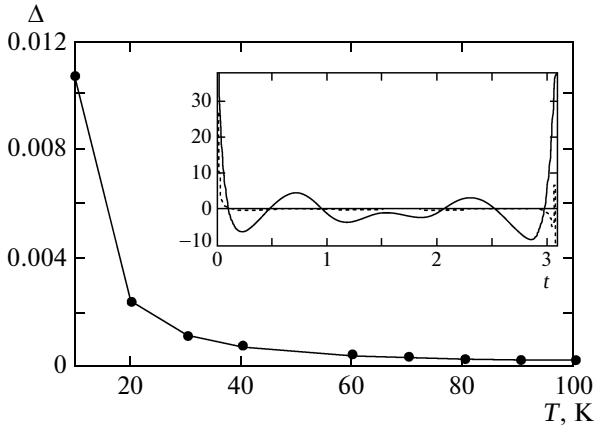

Fig. 3. Dependence of operator $R_y^{0-1}(\pi)$ error on partition number N for a fixed duration of an RF pulse $T = 3.1$. The inset shows the shape of the optimized RF pulse for $N = 200$ ($\Delta = 1.9 \times 10^{-4}$); u_x and u_y are shown by the dotted and solid curves, respectively. The maximum amplitudes at the ends of the time interval $u_x(0) = 42.61$, $u_y(0) = 44.21$, $u_x(3.1) = -61.16$, and $u_y(3.1) = 57.66$ are not shown. The amplitudes and time are measured in units q and $1/q$, respectively.

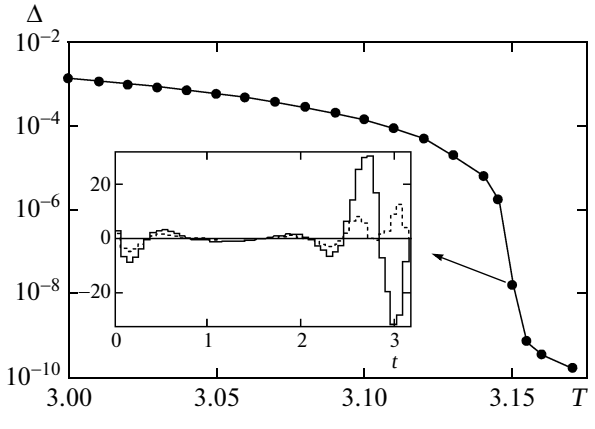

Fig. 4. Dependence of the QFT operator error on the optimized RF pulse duration for $N = 50$. The inset shows the shape of the optimized pulse for $T = 3.15$; u_x and u_y are shown by the dotted and solid curves, respectively. The amplitudes and time are measured in units q and $1/q$, respectively.

$$R_z^{0-1}(\pi) = R_y^{0-1}\left(\frac{\pi}{2}\right) R_x^{0-1}(\pi) R_y^{0-1}\left(-\frac{\pi}{2}\right) \qquad (12)$$

is used. The same QFT operator can be obtained by calculating $u_\alpha(t)$ directly for matrix (11) by the GRAPE method. The calculation results are shown in Fig. 4. It is seen that the minimal QFT time is $T_m \approx 3.15/q$ in this case, which is 1.7 and 3.8 times smaller than the values $5.36/q$ and $12.02/q$, respectively, presented above.

3. TWO-QUTRIT SUM GATE

The SUM gate performs the logical operation [10, 19]

$$\mathrm{SUM}_{12}|m\rangle_1 \otimes |n\rangle_2 = |m\rangle_1 \otimes |m + n(\mathrm{mod}\,3)\rangle_2 \qquad (13)$$

of changing the n state of the second qutrit depending on the m state of the first qutrit. The computation basis in the space of two qutrits is formed by the direct product of one-qutrit bases (2). The SUM gate (13) in this basis will be the 9×9 block matrix

$$\mathrm{SUM}_{12} = \begin{bmatrix} E & 0 & 0 \\ 0 & A & 0 \\ 0 & 0 & A' \end{bmatrix}, \qquad A = \begin{bmatrix} 0 & 0 & 1 \\ 1 & 0 & 0 \\ 0 & 1 & 0 \end{bmatrix}, \qquad (14)$$

where A' is the transposed matrix and E is the unit matrix.

We consider the realization of this gate in the system of two quadrupole nuclei with spin $I = 1$ coupled by the spin–spin interaction (dipole–dipole in anisotropic media) with the Hamiltonian in the RCS,

$$H = -(\omega_1 - \omega_{\mathrm{rf}})I_{1z} - (\omega_2 - \omega_{\mathrm{rf}})I_{2z} + q_1\left(I_{1z}^2 - \frac{2}{3}\right) + q_2\left(I_{2z}^2 - \frac{2}{3}\right) - JI_{1z}I_{2z} + H_{\mathrm{rf}}(t), \qquad (15)$$

$$H_{\mathrm{rf}}(t) = u_x(t)\left(\frac{\gamma_1 I_{1x}}{\gamma_2} + I_{2x}\right) + u_y(t)\left(\frac{\gamma_1 I_{1y}}{\gamma_2} + I_{2y}\right).$$

Here, $\omega_k = \gamma_k B_0$ is the Larmor frequency of spin k, q_k are the corresponding quadrupole constants, and J is the spin–spin interaction constant.

Note that in real systems, as a rule, $J \ll q, \omega$. Consider, for example, the nitrogen nucleus ^{14}N and the deuteron ^{2}H. Both these nuclei have spin $I = 1$. For example, in the solid state in the magnetic field $B_0 = 70$ kOe, we have for the N_2 molecule $\omega_1 \approx 22$ MHz, $q \approx 4$ MHz, and $J \approx 200$ Hz, i.e., $J/q \sim 10^{-4}$. For the heavy water D_2O molecule, $\omega_1 \approx 46$ MHz, $q \approx 200$ kHz, and $J \approx 1$ kHz (interaction between deuterons), and the ratio is $J/q \sim 10^{-2}$. Finally, in [43], the triplet state of a system of two hydrogens in the CH_2 group was used as a qutrit. In this case, the ratio of dipole–dipole constants between groups and inside a group will be about 10^{-1}. These relations between the spin–spin and quadrupole interactions are used below in calculations.

In the case of a weak spin–spin interaction, the SUM gate can be realized with the help of a RF field inducing transitions selective in the quadrupole interaction. The scheme of such a realization has the form [10, 18, 19]

$$\mathrm{SUM}_{12} = (E \otimes F_2)^{-1} P_{12} (E \otimes F_2), \quad (16)$$

where F_2 is the Fourier-transform operator acting on the second spin, and P_{12} is the two-qutrit operator of the controllable phase shift of states with a 9×9 diagonal matrix having matrix elements

$$\langle mn|P_{12}|mn\rangle = \exp\left(i\frac{2\pi}{3}mn\right). \quad (17)$$

The operator P_{12} shifts the phase by an angle depending on the states m and n of qutrits, which can take values of 0, 1, or 2.

Diagonal operator P_{12} (17) can be expressed in terms of operators I_{1z} and I_{2z} [11, 18, 38] as

$$P_{12} = \exp\left(i\frac{2\pi}{3}I_{1z}I_{2z}\right)\exp\left(-i\frac{2\pi}{3}I_{1z}\right) \times \exp\left(-i\frac{2\pi}{3}I_{2z}\right)\exp\left(i\frac{2\pi}{3}\right). \quad (18)$$

The first operator is realized by means of the free evolution of a quantum system with the spin–spin interaction Hamiltonian $H_J = -JI_{1z}I_{2z}$ during time

$$t_J = \frac{2\pi}{3J}. \quad (19)$$

To eliminate the undesirable phase shift caused by the quadrupole interaction [24], the time between the direct and inverse QFTs in (16) should be a multiple of the period $2\pi/q_2$. For this reason, we will round off time t_J (19) to a smaller value corresponding to the duration of an integer of such periods. The second and third operators in (18) perform two additional z rotations through anglers $2\pi/3$ in each spin [20]

$$Z_1 = \exp\left(-i\frac{2\pi}{3}I_{1z}\right), \quad Z_2 = \exp\left(-i\frac{2\pi}{3}I_{2z}\right). \quad (20)$$

These spin-selective operators, which are not transition-selective, can be realized by several transition-selective RF pulses [38]. The common phase factor in (18) does not affect the final result and therefore can be discarded.

For the ratio $J/q \sim 10^{-4}$–10^{-1} chosen above, the SUM gate duration is primarily determined by the strength of the spin–spin interaction and is $T = t_J$ if the duration of local operators is neglected. When the free evolution time is decreased,

$$T = xt_J = x\frac{2\pi}{3J},$$

the required phase difference between states in (18) will not be obtained, gate (14) will be distorted, and

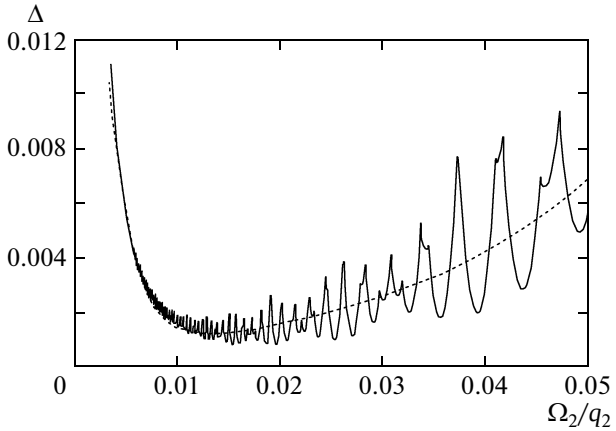

Fig. 5. Error of SUM gate realization by means of quadrupole-splitting-selective rectangular pulses as a function of RF-field amplitude $\Omega_2 = \gamma_2 B_{\mathrm{rf}}$. The parameters of Hamiltonian (15) are $\omega_1 = 60q_2$, $\omega_2 = 20q_2$, $q_1 = 2q_2$, and $J = 10^{-4}q_2$. The dotted curve shows the averaged numerical approximation of the calculated dependence with the help of a sum of three exponentials.

the dependence of this error (6) on the parameter x will be described by the expression

$$\Delta = 1 - \left\{1 - \frac{8}{9}\sin^2\left[\frac{\pi}{3}(1-x)\right]\right\}^2. \quad (21)$$

This expression was obtained by assuming that the Fourier-transform and z-rotation operators are ideal operators that introduce no errors.

We start to analyze the dependence of the accuracy of SUM gate (16) on the physical parameters from the simple case when QFT operators (11) are realized using rectangular quadrupole-splitting-selective RF pulses (5), whereas z rotations (20) are realized by means of the RF-field phase shift. The dependence of error (6) on the RF-field amplitude $\Omega_2 = \gamma_2 B_{\mathrm{rf}}$ is shown in Fig. 5. The error increases at large field amplitudes due to violation of the selectivity of pulses over the quadrupole splitting (this is explained by the action of pulses at large field amplitudes not only on the required transitions but also to a variable degree on all other transitions). On the contrary, a small-amplitude RF field in the presence of detuning $\pm J$ performs rotations with distortions, which also leads to errors. In the case of the combined action of these mechanisms, a minimum is observed at which their influence on the error becomes equal. The dependence of the minimal error on J is shown in Fig. 6.

If the spin–spin interaction is strong enough, the SUM gate can be obtained by direct RF-field excitation of transitions between the states of qutrits con-

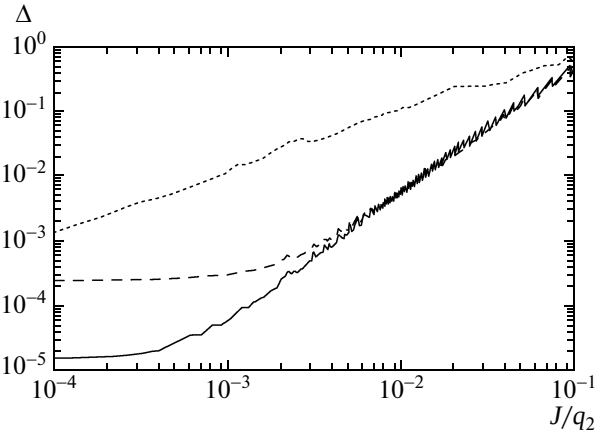

Fig. 6. Error of SUM gate realization as a function of J; the dotted curve shows the minimal error found from the approximating curve in Fig. 5. The error of realization with the help of optimized pulses in the scheme in Fig. 7 is shown by the solid curve for $\omega_1 = 300q_2$, $\omega_2 = 100q_2$ and the dashed curve for $\omega_1 = 60q_2$ and $\omega_2 = 20q_2$. In all cases, $q_1 = 2q_2$.

nected by nonzero elements of matrix (14), i.e., between the following states:

$$\begin{bmatrix} |1\rangle|0\rangle \longrightarrow |1\rangle|1\rangle\ (\lambda_3 \longrightarrow \lambda_4) \\ |1\rangle|1\rangle \longrightarrow |1\rangle|2\rangle\ (\lambda_4 \longrightarrow \lambda_5) \\ |1\rangle|2\rangle \longrightarrow |1\rangle|0\rangle\ (\lambda_5 \longrightarrow \lambda_3) \end{bmatrix}, \quad \begin{bmatrix} |2\rangle|0\rangle \longrightarrow |2\rangle|2\rangle\ (\lambda_6 \longrightarrow \lambda_8) \\ |2\rangle|1\rangle \longrightarrow |2\rangle|0\rangle\ (\lambda_7 \longrightarrow \lambda_6) \\ |2\rangle|2\rangle \longrightarrow |2\rangle|1\rangle\ (\lambda_8 \longrightarrow \lambda_7) \end{bmatrix}. \tag{22}$$

Transitions between energy levels (in parentheses) are performed with the help of selective rotations similar to (4) by π at the corresponding resonance frequency. The pulse sequence for obtaining the gate has the form [38]

$$R_y^{6-7}(\pi) \longrightarrow R_y^{7-8}(\pi) \longrightarrow R_y^{4-5}(\pi) \longrightarrow R_y^{3-4}(\pi). \tag{23}$$

The arrows show the order of succession of pulses in time. This sequence ensures selective rotations not only at the allowed transitions but also at the forbidden 6–8 and 3–5 transitions in (22). The resonance frequencies of RF pulses in (15) will take values of

$$\omega^{6-7} = \omega_2 - q_2 - J, \quad \omega^{7-8} = \omega_2 + q_2 - J, \quad \omega^{4-5} = \omega_2 + q_2, \quad \omega^{3-4} = \omega_2 - q_2. \tag{24}$$

Because close frequencies in (24) differ by J ($J \ll q$), the condition of selective action on the state of the second qutrit will be the smallness of the RF-field amplitude compared to the constant J ($\Omega_2 \ll J$). Therefore, the duration $T_p = \pi/\Omega\sqrt{2}$ (5) of each π-pulse will be much greater than t_J (19).

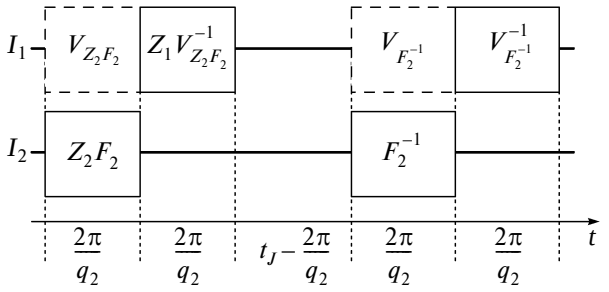

Fig. 7. Scheme of SUM gate realization by means of controllable-phase-shift and QFT operators with correcting gates switched on. The time scale shows the durations of gates and free evolution; time t_J is rounded off to a smaller value to the duration of an integer of periods $2\pi/q_2$.

One of the possibilities of keeping the states of nonresonance transitions unchanged in this SUM gate realization method was pointed out in [44]. It is related to a specific feature of the RF-field action on the nearest nonresonance transitions in the spin system at frequencies differing from the resonance frequencies of pulses (22) by J due to the spin–spin interaction. When the resonance transitions of the second spin rotate at frequency Ω_2, these nonresonance states will rotate at the frequency $\sqrt{2\Omega_2^2 + J^2/2}$, thereby producing an error. However, if the amplitude value is such that upon resonance rotation of the spin through π, the nonresonance states rotate through a multiple of the angle 2π, the computation error will be minimal, as confirmed by our computations [38]. A small error about 10^{-3} remains from parasitic transitions in the first block of SUM matrix (14) at frequencies differing from resonance frequencies (22) by $2J$. By using the relation $\Omega_2 = J/\sqrt{6}$ for the first minimum of the error, we obtain the dependence of the experiment time on J

$$T = 4\sqrt{3}\pi/J. \tag{25}$$

This time is $6\sqrt{3}$ times greater than the minimal time t_J (19).

Based on the results obtained in the previous section, we will try to reduce the error caused by the violated selectivity of RF pulses in the SUM realization methods considered above. For this purpose, we use RF pulses optimized by the GRAPE method. The SUM gate will be realized according to the scheme shown in Fig. 7. In this scheme, the operator of the first QFT is combined with the phase shift operator Z_2 and the optimized RF pulses were calculated for matrices Z_2F_2 and F_2^{-1} at the field frequency $\omega_{rf} = \omega_2$. Because these pulses act nonresonantly on the first spin, we will represent the related error as the result of the action of some corresponding operators $V_{Z_2F_2}$ and $V_{F_2^{-1}}$ on the state of the first qutrit. To eliminate the

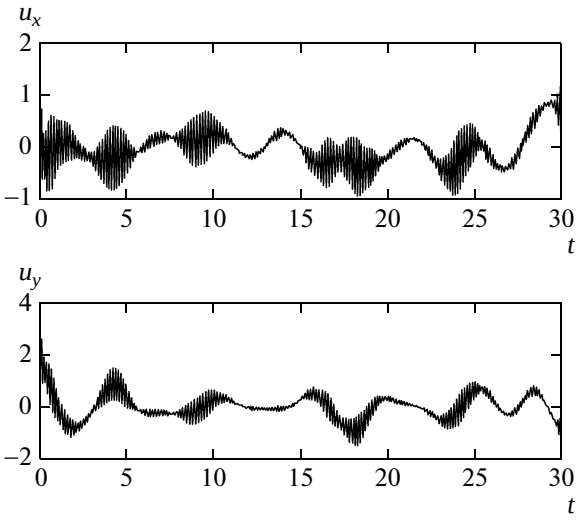

Fig. 8. Shape of optimized RF pulse for realization of the SUM gate calculated for the total matrix of the operator in the 9×9 basis. Parameters of Hamiltonian (15) are $\omega_1 = 60q_2$, $\omega_2 = 20q_2$, $q_1 = 2q_2$, $J = 10^{-1}q_2$, and $\omega_{rf} = \omega_2$. The operation error is $\Delta \sim 10^{-6}$. The amplitudes and time are measured in units q_2 and $1/q_2$, respectively.

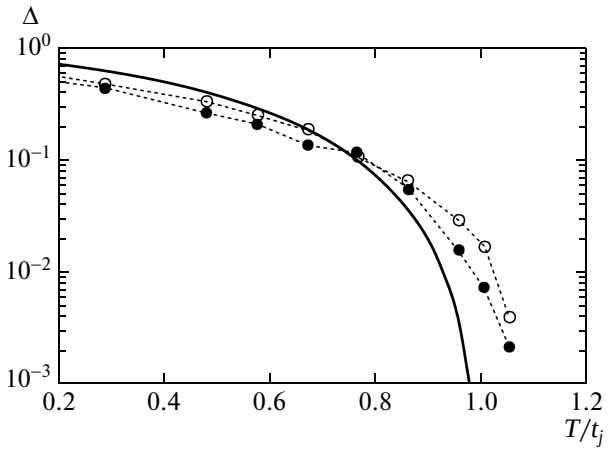

Fig. 9. Dependence of SUM gate realization error on the duration of the optimized pulse calculated for the entire 9×9 matrix. Calculations are performed with parameters $\omega_1 = 60q_2$, $\omega_2 = 20q_2$, $J = 10^{-1}q_2$ (○) and $\omega_1 = 6q_2$, $\omega_2 = 2q_2$, $J = 10^{-2}q_2$ (●). In both cases, $q_1 = 2q_2$. The solid curve is the theoretical estimate by (21).

error caused by $V_{Z_2F_2}$ and $V_{F_2^{-1}}$, we apply optimized pulses at the frequency of the first spin ($\omega_{rf} = \omega_1$) performing operations $Z_1 V_{Z_2F_2}^{-1}$ and $V_{F_2^{-1}}^{-1}$. These pulses also will affect the second spin, but because the system parameters are selected so that $\gamma_1 > \gamma_2$, this action will be insignificant and we will not switch additional correcting pulses on the second spin. All the optimized pulses for the above-mentioned operators were calculated for individual spins in the 3×3 basis, and then their action on total system (15) was simulated in the 9×9 basis. To eliminate the phase shift caused by quadrupole interaction, the duration of each pulse was set equal to $2\pi/q_2$.

The error of the SUM gate realized by the scheme in Fig. 7 as a function of the spin–spin interaction between qutrits for two values of $|\omega_1 - \omega_2|$ is shown in Fig. 6. For small J, the error was considerably reduced on passing from rectangular to optimized RF pulses. As the value of J was increased, the monotonic increase in the error $\Delta \sim J^2$ was observed beginning from $J/q \geq 10^{-3}$. The increasing contribution to the error, independent of $|\omega_1 - \omega_2|$, is caused by the violation of resonance conditions for quadrupole-splitting-selective RF pulses by $\pm J$; i.e., this error has the same nature as that in Fig. 5 at small amplitudes of rectangular RF pulses. The optimization performed for the switched off spin–spin interaction does not eliminate this part of the error. Note that it can be reduced at very large values of $|\omega_1 - \omega_2|$ by applying short π pulses to the first spin in the middle of operators acting on the second spin.

To eliminate the error caused by the spin–spin interaction and the error related to the nonselectivity of RF pulses at small $|\omega_1 - \omega_2|$, the optimized pulse should be calculated immediately in the 9×9 basis either for individual operators (scheme in Fig. 7) or directly for SUM gate matrix (14). The latter is preferable when all the parameters have close values. An example of such calculation is shown in Fig. 8. The control RF field with such a complex shape used in simulations ensures reduction in the error down to $\Delta \sim 10^{-6}$. The oscillations of components $u_x(t)$ and $u_y(t)$ of the RF-field amplitudes at a high frequency on the order of $|\omega_1 - \omega_2|$ for the pulse frequency $\omega_{rf} = \omega_2$ show that the GRAPE algorithm selects a multifrequency RF field acting simultaneously on both spins near the resonance. We repeated calculations for different gate durations (in this case, the condition of multiplicity to $2\pi/q_2$ was not imposed) and two values of J. The results for the error are shown in Fig. 9, where the limiting dependence calculated by formula (21) is also presented. We can see from Fig. 9 that numerical calculations of the minimal time performed by the GRAPE method give a value close to the boundary value $T = t_J$ (19). For $T \lesssim 0.7t_J$, the optimized gate has a smaller error, whereas for $T \gtrsim 0.7t_J$, the error was larger than theoretical estimate (21), although it was quantitatively close to the latter. These discrepancies can be explained either by the fact that the real parameters of the quantum system were used instead of the limiting parameters used in the derivation of (21) or by the insufficient calculation accuracy due to poor convergence of the algorithm for $T \sim t_J$. The fact of matter

is that, to reproduce multifrequency oscillations (Fig. 8), the time interval is divided into many segments. Therefore, due to the slow convergence, the calculation time increases up to several days and the calculation should be stopped after many iterations of the algorithm (about 5×10^4) rather than after the achievement of the desired accuracy.

4. CONCLUSIONS

We have studied the dependences of errors on the duration of one- and two-qutrit gates realized on quadrupole nuclei with spin $I = 1$ by means of simple and composite selective RF pulses and RF pulses optimized by the GRAPE method. The main goal of our numerical simulations was to propose recommendations on the reduction gate times.

Our calculations have shown that, for the same error, the duration of selective rotations obtained by using a simple RF pulse is considerably greater than the duration of composite and optimized RF pulses. The duration of a composite selective pulse can be made close to the optimal one by using a sequence of many high-power nonselective RF pulses. With an optimized RF pulse, the same accuracy can be achieved with a smaller RF-field amplitude at a small partition number. However, the minimal operation time is preserved in this case as well because it is determined by interaction H_q, which ensures the nonequidistance of the levels required for the selective action of H_{rf} and, finally, the realization of the universal unitary operator. This conclusion is consistent with the general quantum system control theory [45].

Note that some particular operations with the help of a strong RF field can be performed for an arbitrarily short time, for example, the spin rotation by a field arbitrarily varying in time. Among such particular operations are those produced by pulses inverting the states of two levels from three pulses and calculated by the GRAPE optimization method in [41] because in this case the phase of the state of the third level in neglected, whereas to create a gate for the selective control of the states of two qutrit levels, the phase of the third level state should be zero. Otherwise, it will be impossible, for example, to perform the QFT of a qutrit by scheme (11).

Our study has shown that the optimized RF pulse, calculated directly for the matrix of the QFT operator, is considerably shorter than the same operator composed of selective-rotation operators realized by optimized RF pulses. Therefore, the representation of the QFT operator by the product of selective rotations is not optimal in time. Note that a similar conclusion was made earlier [46] for multiqubit systems of spins $I = 1/2$ controlled by spin-selective RF fields.

The numerical simulation of different methods for realization of the SUM gate has led to the following conclusions. The method using weak spin–spin-interaction-selective RF pulses is simpler, but because small RF-field amplitudes are needed, the total time of the experiment increases; i.e., this method is not time-optimal. In another method based on strong quadrupole-interaction-selective RF pulses, the sequence of pulses is much more complicated and the free evolution time of the system is added, but the change in the selectivity conditions makes it possible to increase the RF-field amplitude by tens of times. Therefore, the duration of the experiment can be reduced by several times.

Calculation of the SUM gate by the numerical optimization method has shown that this method is time-optimal in systems with a weak spin–spin interaction ($J/q \ll 1$), when the minimal time is determined by the value of J and is close to t_J (19). In this case, the optimized RF pulse with the same duration makes it possible to reduce the error by an order of magnitude. We have found that for close values of parameters ($J/q \sim 10^{-2}$–10^{-1}), it is preferable to calculate the optimized RF pulse for the 9×9 matrix of the SUM operator as a whole, whereas in the case of a very weak spin–spin interaction ($J/q \sim 10^{-4}$–10^{-3}), sufficient accuracy can be achieved by calculating optimized RF pulses for one-qutrit operators with 3×3 matrices, which reduces the calculation time and provides a greater universality. The latter result is important for further quantum computations in multiqutrit systems.

ACKNOWLEDGMENTS

This work was supported by the Russian Foundation for Basic Research (project no. 09-07-00138) and the Dynasty Foundation.

REFERENCES

1. T. C. Ralph, K. J. Resch, and A. Gilchrist, Phys. Rev. A: At., Mol., Opt. Phys. **75**, 022313 (2007).
2. B. P. Lanyon, M. Barbieri, M. P. Almeida, T. Jennewein, T. C. Ralph, K. J. Resch, G. J. Pryde, J. L. O'Brien, A. Gilchrist, and A. G. White, Nat. Phys. **5**, 134 (2009).
3. D. Aharonov, W. van Dam, J. Kampe, Z. Landau, S. Lloyd, and O. Regev, SIAM J. Comput. **37** (1), 166 (2007); arXiv:quant-ph/0405098.
4. B. A. Chase and A. J. Landahl, arXiv:quant-ph//0802.1207.
5. K. G. H. Vollbrecht and J. I. Cirac, Phys. Rev. Lett. **100**, 010501 (2008).
6. D. Nagaj and P. Wocjan, Phys. Rev. A: At., Mol., Opt. Phys. **78**, 032311 (2008).
7. D. Nagaj, arXiv:quant-ph/1002.0420.
8. J. Cai, A. Miyake, W. Dür, and H. J. Briegel, Phys. Rev. A: At., Mol., Opt. Phys. **82**, 052309 (2010).
9. A. Muthukrishnan and C. R. Stroud, Jr., Phys. Rev. A: At., Mol., Opt. Phys. **62**, 052309 (2000).
10. S. D. Bartlett, H. de Guise, and B. C. Sanders, Phys. Rev. A: At., Mol., Opt. Phys. **65**, 052316 (2002).

11. V. E. Zobov, V. P. Shauro, and A. S. Ermilov, Pis'ma Zh. Eksp. Teor. Fiz. **87** (6), 385 (2008) [JETP Lett. **87** (6), 334 (2008)].
12. B. Tamir, Phys. Rev. A: At., Mol., Opt. Phys. **77**, 022326 (2008).
13. A. Kushnerov, *Ternary Digital Techniques: Retrospective and Contemporaneity* (Ben-Gurion University Press, Bersabee, Israel, 2005) [in Russian].
14. V. E. Zobov and D. I. Pekhterev, Pis'ma Zh. Eksp. Teor. Fiz. **89** (5), 303 (2009) [JETP Lett. **89** (5), 260 (2009)].
15. D. Gottesman, Lect. Notes Comput. Sci. **1509**, 302 (1999).
16. D. Gottesman, A. Kitaev, and J. Preskill, Phys. Rev. A: At., Mol., Opt. Phys. **64**, 012310 (2001).
17. A. Yu. Vlasov, J. Math. Phys. **43**, 2959 (2002).
18. J. Daboul, X. Wang, and B. C. Sanders, J. Phys. A: Math. Gen. **36**, 2525 (2003).
19. A. B. Klimov, R. Guzman, J. C. Retamal, and C. Saavedra, Phys. Rev. A: At., Mol., Opt. Phys. **67**, 062313 (2003).
20. Ch. Slichter, *Principles of Magnetic Resonance* (Springer, Heidelberg, 1978; Mir, Moscow, 1981).
21. R. Das, A. Mitra, V. Kumar, and A. Kumar, Int. J. Quantum Inf. **1**, 387 (2003).
22. A. K. Khitrin and B. M. Fung, J. Chem. Phys. **112**, 6963 (2000).
23. V. L. Ermakov and B. M. Fung, Phys. Rev. A: At., Mol., Opt. Phys. **66**, 042310 (2002).
24. R. Das and A. Kumar, Phys. Rev. A: At., Mol., Opt. Phys. **68**, 032304 (2003).
25. R. Das and A. Kumar, Appl. Phys. Lett. A **89**, 024107 (2006).
26. T. Gopinath and A. Kumar, J. Magn. Reson. **193**, 2 (2008); arXiv:quant-ph/0909.4034.
27. A. K. Khitrin, H. Sun, and B. M. Fung, Phys. Rev. A: At., Mol., Opt. Phys. **63**, 020301 (2001).
28. A. K. Khitrin and B. M. Fung, Phys. Rev. A: At., Mol., Opt. Phys. **64**, 032306 (2001).
29. V. E. Zobov and V. P. Shauro, Pis'ma Zh. Eksp. Teor. Fiz. **86** (4), 260 (2007) [JETP Lett. **86** (4), 230 (2007)].
30. V. E. Zobov and V. P. Shauro, Zh. Eksp. Teor. Fiz. **135** (1), 10 (2009) [JETP **108** (1), 5 (2009)].
31. T. Vosegaard, C. Kehlet, N. Khaneja, S. J. Glaser, and N. Chr. Nielsen, J. Am. Chem. Soc. **127**, 13768 (2005).
32. N. Khaneja, T. Reiss, C. Kehlet, T. Schulte-Herbrüggen, and S. J. Glaser, J. Magn. Reson. **172**, 296 (2005).
33. J.-S. Lee, R. R. Regatte, and A. Jerschow, J. Chem. Phys. **129**, 224510 (2008).
34. I. I. Maximov, J. Salomon, G. Turinici, and N. Chr. Nielsen, J. Chem. Phys. **132**, 084107 (2010).
35. H. Kampermann and W. S. Veeman, J. Chem. Phys. **122**, 214108 (2005).
36. D. O. Soares-Pinto, L. C. Celeri, R. Auccaise, F. F. Fanchini, E. R. deAzevedo, J. Maziero, T. J. Bonagamba, and R. M. Serra, Phys. Rev. A: At., Mol., Opt. Phys. **81**, 062118 (2010).
37. E. M. Fortunato, M. A. Pravia, N. Boulant, G. Teklemariam, T. F. Havel, and D. G. Cory, J. Chem. Phys. **116**, 7599 (2002).
38. V. P. Shauro, D. I. Pekhterev, and V. E. Zobov, Izv. Vyssh. Uchebn. Zaved., Fiz., No. 6, 41 (2007) [Russ. Phys. J. **50** (6), 566 (2007)].
39. C. A. Ryan, C. Negrevergne, M. Laforest, E. Knill, and R. Laflamme, Phys. Rev. A: At., Mol., Opt. Phys. **78**, 012328 (2008).
40. P. Rebentrost and F. K. Wilhelm, Phys. Rev. B: Condens. Matter **79**, 060507 (2009).
41. F. Motzoi, J. M. Gambetta, P. Rebentrost, and F. K. Wilhelm, Phys. Rev. Lett. **103**, 110501 (2009).
42. A. S. Ermilov and V. E. Zobov, Opt. Spektrosk. **103** (6), 994 (2007) [Opt. Spectrosc. **103** (6), 969 (2007)].
43. T. Gopinath and A. Kumar, Phys. Rev. A: At., Mol., Opt. Phys. **73**, 022326 (2006).
44. G. P. Berman, G. D. Doolen, G. V. Lopez, and V. I. Tsifrinovich, Phys. Rev. A: At., Mol., Opt. Phys. **61**, 042307 (2000).
45. N. Khaneja, R. Brockett, and S. J. Glaser, Phys. Rev. A: At., Mol., Opt. Phys. **63**, 032308 (2001).
46. T. Schulte-Herbrüggen, A. Spörl, N. Khaneja, and S. J. Glaser, Phys. Rev. A: At., Mol., Opt. Phys. **72**, 042331 (2005).

Translated by M. Sapozhnikov